

Article

Mechanical Properties of Thermally Annealed Cu/Ni and Cu/Al Multilayer Thin Films: Solid Solution vs. Intermetallic Strengthening

Yang Zhou and Junlan Wang *

Department of Mechanical Engineering, University of Washington, Seattle, WA 98195, USA

* Correspondence: junlan@u.washington.edu

Abstract: In this study, Cu/Ni and Cu/Al multilayers, with individual layer thickness varying from 25 nm to 200 nm, and co-sputtered Cu-Ni and Cu-Al single layer films were deposited at room temperature via magnetron sputtering and further annealed from 100 °C to 300 °C. The mechanical and microstructural properties of the as-deposited and annealed samples were characterized by nanoindentation, x-ray diffraction, and scanning electron microscopy. Both multilayer systems exhibit an increase in hardness with increasing annealing temperature. However, the Cu/Ni system shows a gradual and moderate hardness increase (up to 30%) from room temperature to 300 °C, while the Cu/Al system displays a sharp hardness surge (~150%) between 125 °C and 200 °C. The co-sputtered Cu-Ni and Cu-Al samples consistently demonstrate higher hardness than their multilayered counterparts, albeit with distinctly different temperature dependence—the hardness of Cu-Ni increases with annealing temperature while Cu-Al maintains a constant high hardness throughout the entire temperature range. The distinct thermal strengthening mechanisms observed in the two metallic multilayer systems can be ascribed to the formation of solid solutions in Cu/Ni and the precipitation of intermetallic phases in Cu/Al. This study highlights the unique advantage of intermetallic strengthening in metallic multilayer systems.

Keywords: metallic multilayer; Cu/Ni; Cu/Al; thermal strengthening; intermetallic strengthening



Citation: Zhou, Y.; Wang, J. Mechanical Properties of Thermally Annealed Cu/Ni and Cu/Al Multilayer Thin Films: Solid Solution vs. Intermetallic Strengthening. *Metals* **2024**, *14*, 256. <https://doi.org/10.3390/met14030256>

Academic Editors: Ahmed Al-Kattan, Randi Holmestad and Catalin Constantinescu

Received: 31 December 2023

Revised: 8 February 2024

Accepted: 19 February 2024

Published: 21 February 2024



Copyright: © 2024 by the authors. Licensee MDPI, Basel, Switzerland. This article is an open access article distributed under the terms and conditions of the Creative Commons Attribution (CC BY) license (<https://creativecommons.org/licenses/by/4.0/>).

1. Introduction

Metallic multilayers refer to thin films and coatings composed of alternating layers of two or more different metals. In contrast to their bulk counterparts, metallic multilayers offer some extraordinary properties, including but not limited to superior mechanical strength (e.g., up to ½ of the theoretical strength), high corrosion and radiation resistance, and enhanced thermal stability [1–4]. The remarkable mechanical strength observed in metallic multilayers can be attributed to a combination of factors such as layer thickness [5], interface structure [6], deposition temperature [7], and thermal annealing conditions [8,9]. These unique attributes make metallic multilayers highly promising for various applications, offering a spectrum of desirable characteristics not easily achievable in their bulk counterparts.

The number of interfaces and the corresponding layer thickness can affect the metallic multilayer strength by controlling the dislocation motions. For multilayers with an individual layer thickness of 50 nm and greater, strengthening occurs by dislocation pile-up at the layer interfaces which can be explained by the Hall–Petch relation [10–13]. When the layer thickness is between 10 and 50 nm, due to strong repulsion among like-sign coplanar dislocations, the multilayer strengthening can be explained by confined layer slip (CLS) [14–17], involving the movement of a single dislocation loop parallel to the interface within individual layers. The multilayer strength approaches the theoretical value when the layer thickness is around 5 nm. At this thickness scale, the strength of multilayers is affected by coherency stress, misfit dislocations, moduli differences, texture, and chemical

intermixing along the interface [10,13]. The peak strength is determined by the stress needed to transmit a single dislocation across the interface.

In addition to the layer thickness, the crystallography of layers also affects the multilayer strength. For two materials sharing the same crystal structure, such as Cu/Ni multilayers, the strengthening mechanism can be ascribed to the coherency stress at the interfaces [18,19]. For multilayer systems which are composed of different crystal structures, such as Cu/Nb multilayers, the different crystal structures at two sides of the interface may lead to discontinuity of the slip system and different slip vectors. The flow strength is determined by the transmission of dislocation from one material to another [20,21]. However, the original crystal structure of the individual material may be changed when the layer thickness is sufficiently small. For example, in Ag/Fe multilayers, phase transformation in Fe from BCC to FCC occurs when the layer thickness reaches 5 nm [22]. Also, a superlattice structure has been observed in Cu/Ni multilayer thin films when the layer thickness is smaller than 5 nm [23]. The high-density nanotwins and coherent layer interfaces in highly textured multilayers led to a significant enhancement of the multilayer strengths and delayed the onset of softening.

In addition to the aforementioned mechanisms, the mechanical properties of metallic multilayers can be affected by deposition temperature and heat treatment conditions as well. When a Ti/Ni multilayer with 25 nm individual layer thickness was deposited from room temperature to 500 °C, the multilayer hardness was observed to increase with deposition temperature. This rise in hardness can be attributed to various strengthening mechanisms, including texture strengthening, low-temperature grain boundary relaxation, and high-temperature alloying [7].

Annealed Ti/Ni multilayers show a coupled size and temperature strengthening behavior. For multilayers with a small layer thickness (<25 nm), the multilayer hardness was observed to continuously increase with annealing temperatures up to 500 °C. Conversely, for a larger layer thickness, the multilayer hardness was observed to first increase with annealing temperatures up to 300–400 °C, after which it exhibited a decrease [8,9]. At low annealing temperatures, the increase in hardness was attributed to grain boundary relaxation, while at high annealing temperatures, the competition between heat-induced alloy strengthening and grain growth softening played a significant role.

In some special metallic multilayer systems, such as Cu/Al, high hardness was usually observed in both as-deposited [24] and annealed samples [25] beyond that predicted by the layer thickness effect. The strengthening was attributed to both the high-density nanotwins and stacking fault as well as the negative enthalpy that led to the intermixing and alloying at the interface region [24]. The strengthening in the annealed Cu/Al multilayers was attributed to interface alloying, reduced layer thickness, and the effect of grain size [25].

Driven by the distinctive advantages of metallic multilayers, and the insights gained from thermal–mechanical strengthening mechanisms, this study focuses on investigating two model multilayer systems: Cu/Ni and Cu/Al. The rationale behind selecting these specific systems lies in the intriguing and markedly different phase diagrams in the corresponding Cu-Ni and Cu-Al alloys, offering two unique avenues for exploration of alloying-based strengthening mechanisms in metallic multilayers.

Cu-Ni, characterized as a simple isomorphous system, exhibits a suggested spinodal decomposition of the FCC phase below 350 °C [26]. The up to 100% mutual solubility of Cu and Ni provides a wide composition range for studying their intermixing effect on the mechanical properties of the resulting alloys due to substitutional alloying. On the other hand, the Cu-Al system presents a different scenario. Despite Al's intrinsically soft and ductile nature, its combination with Cu at different atomic ratios leads to the formation of several Cu-Al intermetallic compound phases. Particularly within the low-temperature range from 150 °C to 300 °C, various intermetallic compounds emerge, including the γ_2 phase (Cu₉Al₄): 69.2 atm% Cu; the δ phase (Cu₃Al₂/Al₂Cu₃): 60.0 atm% Cu; the ζ_2 phase (Cu₄Al₃): 57.1 atm% Cu; the η_2 phase (CuAl): 50.0 atm% Cu; and the θ phase (CuAl₂): 33.3 atm% Cu [27]. The abundant intermetallic phases in Cu-Al add a layer of complexity,

rendering thermally annealed Cu-Al a particularly interesting and potentially stronger alloy compared to annealed Cu-Ni, thus highlighting the unique advantages of intermetallic strengthening.

In the realm of metallic multilayers, previous investigations into Cu/Ni multilayers have predominantly attributed the observed strengthening mechanisms to the interplay of layer thickness and coherency stress at interfaces [7,16,23,28,29]. The layer thickness effect, as elucidated by these studies, underscores the significance of the physical dimensions of individual layers in determining the mechanical properties of the multilayer structure. Additionally, the coherency stress at the interface plays a pivotal role, contributing to the enhanced mechanical strength in Cu/Ni multilayers.

In a distinct contrast, the mechanical behavior of Cu/Al multilayers reveals a more intricate scenario. While the layer thickness effect remains an important factor, influencing the overall strength of the multilayer [25,30], the additional dimension of intermetallic phases introduces a new layer of complexity. Unlike the singular focus on layer thickness in the Cu/Ni multilayers, Cu/Al multilayers undergo phase transformations of intermetallic phases. This phenomenon provides an additional strengthening mechanism that goes beyond the conventional layer thickness effect.

The unique exploration undertaken in this study aims to delve into a comparative analysis of thermally annealed Cu/Ni and Cu/Al multilayers. This comparative approach serves as a valuable endeavor to unravel the distinct thermal strengthening mechanisms inherent in these two metallic multilayer systems upon annealing—substitutional solid solution formation at the Cu/Ni interfaces versus the precipitation of intermetallic phases at the Cu/Al interfaces. Through a systematic examination of these systems in a controlled experimental setting, this research seeks to shed light on the differences between two distinct alloy strengthening mechanisms and their respective contribution to the overall mechanical strength of the multilayer systems.

2. Experimental Details

Cu/Ni and Cu/Al multilayers were prepared with an Orion 5 UHV magnetron sputtering system (AJA International, Inc., Hingham, MA, USA), operating at a base vacuum of $\sim 1 \times 10^{-8}$ mbar. Employing a single-crystal (100) Si wafer as the substrate for all samples, the deposition process involved the use of Cu (99.995%), Ni (99.995%), and Al (99.999%) for direct current (DC) sputtering. A deposition power of 100 W and background Ar pressure of 2 mTorr were consistently applied across all multilayer depositions. To enhance adhesion, a thin titanium layer (~ 10 nm) deposited from a Ti (99.995%) target served as a bonding layer between the Cu/Ni multilayers and the Si substrate. This precaution was essential to prevent spontaneous delamination of Cu/Ni multilayers from the substrate, as established by prior research [31].

The Cu/Ni multilayers featured individual layer thicknesses from 25 to 200 nm, while the Cu/Al had individual thicknesses ranging from 25 to 100 nm. The thickness ratio between adjacent layers was consistently maintained at 1 to 1. The overall thickness of each multilayer sample varied from 1 to 2 μm . For comparative analysis, Cu-Ni and Cu-Al co-sputtered samples, each 500 nm thick, were also prepared. This involved adjusting the deposition power of (Cu, Ni) and (Cu, Al) to achieve the nominal 1:1 atomic ratio between the two metal elements. Post deposition, selected samples underwent vacuum annealing for 2 h in a muffle furnace (Lindberg Blue M, Thermo Fisher Scientific, Greenville, NC, USA) at temperatures ranging from 100 °C to 300 °C.

The crystallinity of both as-deposited and annealed samples was studied by x-ray diffraction (XRD) using a Bruker D8 Discover (Bruker, Billerica, MA, USA) with Cu K α radiation. The sample cross-section morphologies were characterized by scanning electron microscopy (SEM) on a FEI Sirion XL30 (Thermo Fisher Scientific, Greenville, NC, USA). Nanoindentation was conducted using a Hysitron Ubi1 nanoindenter (Bruker Nano Surfaces, Minneapolis, MN, USA) with a Berkovich tip to characterize the hardness of all samples. Indentation was performed in the direction perpendicular to the multilayer

surface under load control. A trapezoid load function with 10 s loading, 5 s holding, and 10s unloading was used for all the testing. To avoid substrate effects, the indentation depth was controlled below 15% of the overall film thickness. The hardness was calculated by dividing the maximum load by the contact area following the standard Oliver and Pharr method [32]. Each sample underwent at least 60 indentations at varying loads to ensure repeatability and reliability of the results.

3. Results and Discussions

3.1. SEM Morphology of As-Deposited Samples

Cross-sectional SEM imaging showed well-defined layered structures in the as-deposited Cu/Ni and Cu/Al multilayers, and columnar structures in their corresponding co-sputtered counterparts.

Figure 1 presents the cross-sectional morphologies of three as-deposited Cu/Ni multilayer samples with layer thicknesses of 200, 100, and 25 nm, respectively, along with one co-sputtered Cu-Ni sample. The multilayer samples reveal highly textured layer-by-layer structures. In Figure 1a,b, the 200 nm and 100 nm layer thickness samples display distinct columnar structures within the Ni layers. The columnar structure is less evident in the 25 nm sample due to its reduced layer thickness. The Cu layers exhibit a less defined grain structure attributed to their ductile deformation during the fracturing process. The entire co-sputtered Cu-Ni film in Figure 1d shows a columnar structure extending through the entire sample film's thickness.

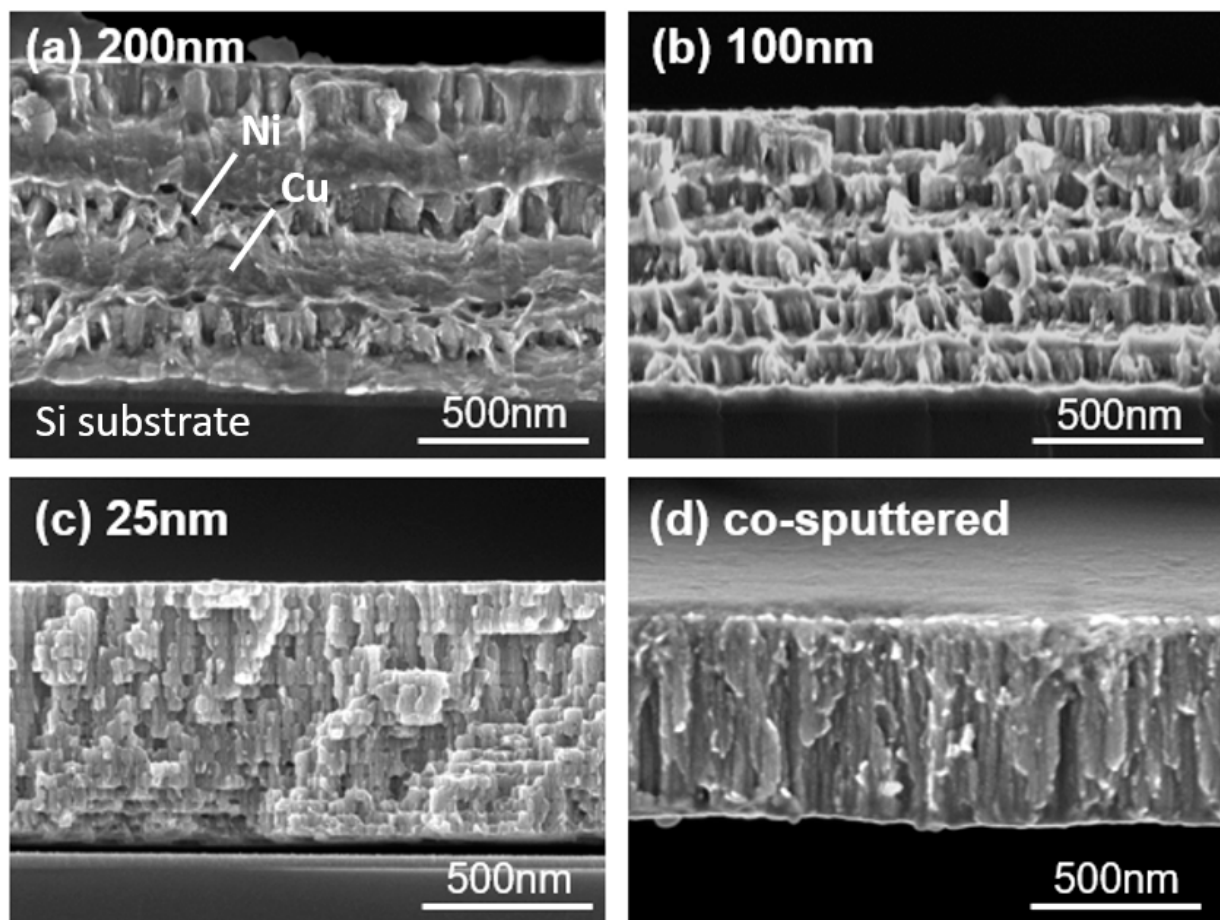


Figure 1. Cross-sectional SEM images of as-deposited Cu/Ni samples with layer thickness of (a) 200 nm, (b) 100 nm, and (c) 25 nm as well as a co-sputtered Cu-Ni sample (d).

Figure 2 shows cross-sectional morphologies for three as-deposited Cu/Al samples, with layer thicknesses of 100, 50, and 25 nm, respectively, along with one co-sputtered Cu-Al sample. The multilayer samples show well-defined layer-by-layer structures with the darker layers corresponding to Al and the brighter layers to Cu. The distinct contrast arises from the higher atomic number of Cu, causing it to scatter more electrons back towards the detector compared to the lighter Al atoms. As a result, Cu appears brighter in the SEM images. However, it is essential to note that the high ductility of both the Cu and Al layers led to significant plastic deformation when the samples were fractured for cross-sectional imaging. The plastic deformation obscured the microstructure, making it challenging to discern fine details in the SEM images of the fractured samples. Meanwhile, the cross-sectional view of the Cu-Al co-sputtered sample in Figure 2d reveals a well-defined columnar structure, adding a layer of clarity to the microstructure comparison.

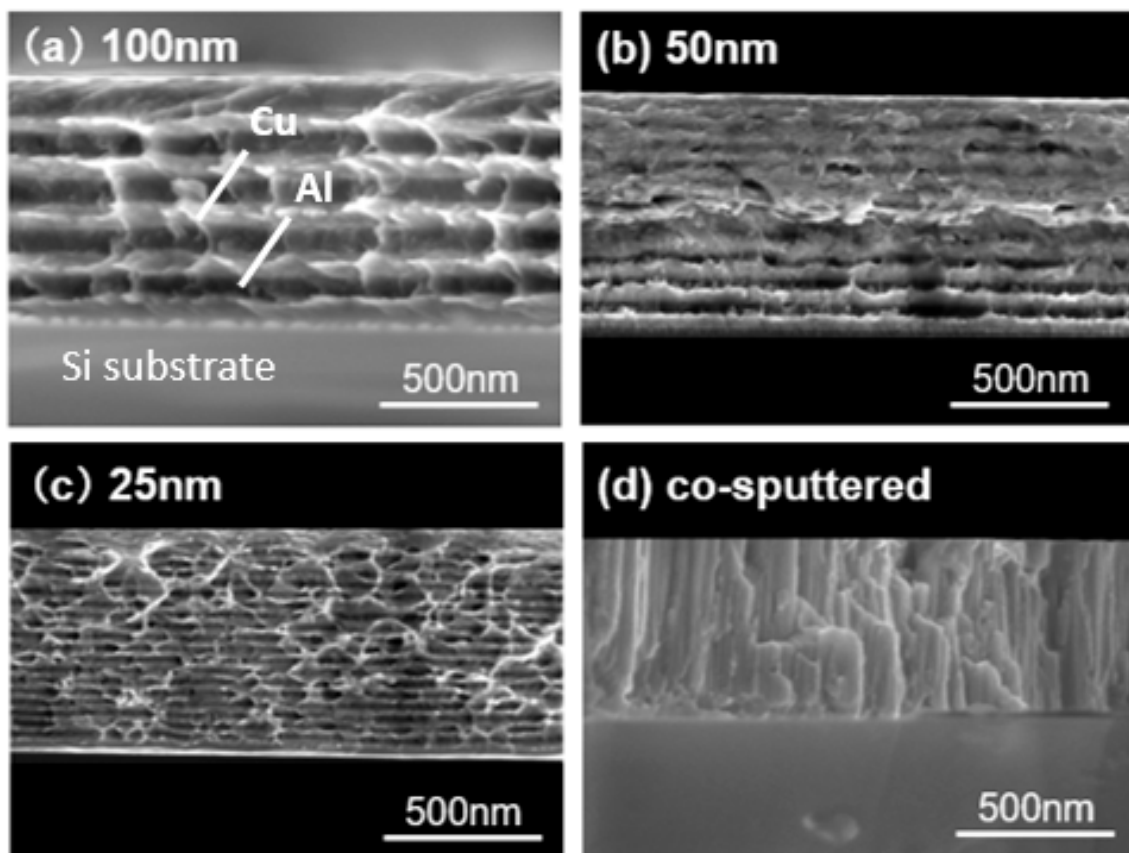


Figure 2. Cross-sectional SEM images of as-deposited Cu/Al multilayer samples with layer thickness of (a) 100 nm, (b) 50 nm and (c) 25 nm, as well as a co-sputtered Cu-Al sample (d).

The observed columnar structure arrangements in the co-sputtered samples in Figures 1d and 2d, contrasting with the layered structure and plastic deformation in their multilayered counterparts, underscore the impact of the deposition methods on the resultant microstructure of the Cu/Ni and Cu/Al multilayers.

3.2. Hardness

The hardness of the Cu/Ni and Cu/Al multilayers, along with that of the co-sputtered samples, was investigated by nanoindentation, and distinctively different strengthening trends were observed. Figure 3 shows the hardness as a function of annealing temperature and layer thickness for both systems. In the as-deposited samples, there is a noticeable increase in hardness as the layer thickness decreases, consistent with the findings in the existing literature attributed to layer interface strengthening [6]. Both the Cu/Ni and

Cu/Al multilayers exhibit an increase in hardness with increasing annealing temperature, yet with distinct trends and magnitudes. The co-sputtered samples consistently display higher hardness compared to the multilayer samples across the entire temperature range for both systems, although with different patterns.

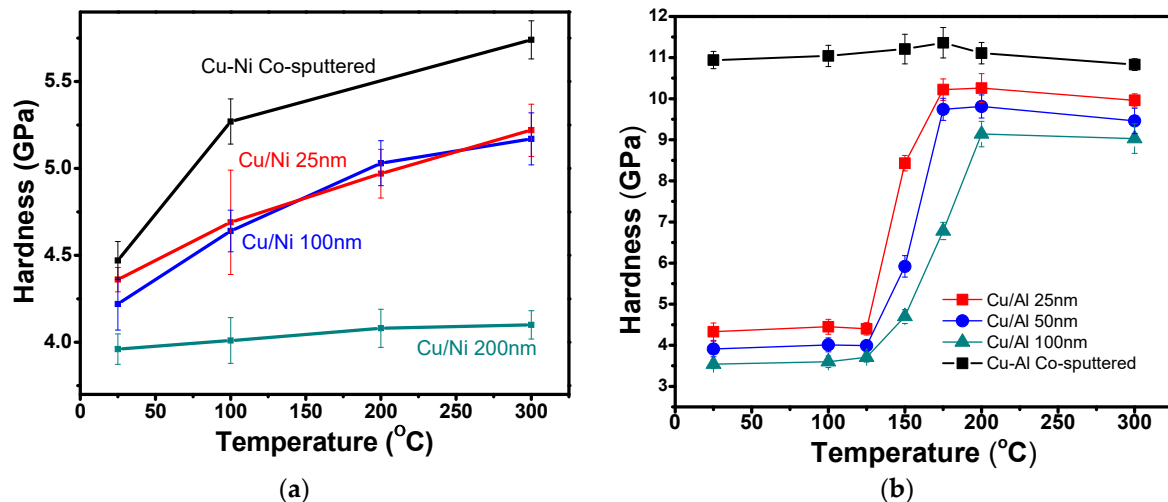


Figure 3. The hardness of (a) Cu/Ni multilayer and co-sputtered Cu-Ni, and (b) Cu/Al multilayer and co-sputtered Cu-Al thin films with different annealing temperatures and different layer thicknesses.

As shown in Figure 3a, the Cu/Ni samples display a gradual and consistent increase in hardness from the as-deposited state to the 300 °C annealed state. Even at the highest annealing temperature of 300 °C, the hardness increase remains moderate (<30%) compared to the as-deposited condition. The hardness increase is more pronounced in thinner layers (e.g., 25 and 100 nm) and co-sputtered samples.

In Figure 3b, Cu/Al samples show a remarkable hardness surge (~150%) within a narrow temperature range (125 °C to 175 °C for the 25 and 50 nm layers, and 125 °C to 200 °C for the 100 nm layers). Below 125 °C there is no visible hardness change with respect to temperature. The multilayers' hardness plateaus after 175 °C (25 and 50 nm layers) and 200 °C (100 nm layer). The co-sputtered Cu-Al sample maintains a consistently high hardness (~11 GPa) throughout the entire temperature range, in stark contrast to the behavior of co-sputtered Cu-Ni, whose hardness is only slightly higher than the multilayered Cu/Ni at room temperature and continues to increase with annealing temperature.

3.3. XRD Spectra

XRD was performed to characterize the microstructure and phase transformation of both systems upon annealing. Figure 4a presents the XRD spectra of the as-deposited Cu/Ni multilayers and co-sputtered Cu-Ni samples. Both Cu and Ni exhibit an FCC structure with prominent peaks for Cu (111), Ni (111), Cu (200), and Ni (200). Analysis of different layer thicknesses revealed a slightly reduced distance between Cu (111) and Ni (111) peaks in the 25 nm layer sample. The decreased peak distance is probably due to distortion of the lattice at each layer interface. The larger number of interfaces in the 25 nm layer thickness sample are expected to result in a higher amount of distortion and subsequent residual stress. Previous work showed that as the layer thickness reduced from 100 nm to 25 nm, the residual stress in the Ni layers increased from 0.88 GPa to 1.45 GPa [31]. For the Cu-Ni co-sputtered sample, the Cu and Ni peaks—Cu (111) and Ni (111), Cu (200) and Ni (200)—merge between their original positions in the thicker layers, indicating a new FCC structure with a lattice constant in between those of Cu and Ni.

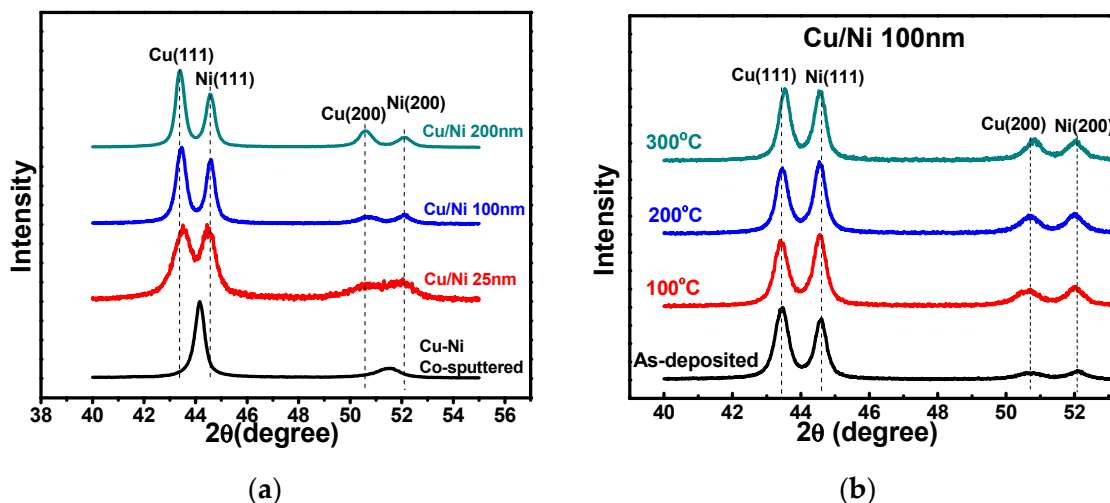


Figure 4. XRD spectra for Cu/Ni multilayer samples: (a) as-deposited multilayers with different layer thickness (including co-sputtered), and (b) 100 nm layer thickness samples at different annealing temperatures.

Figure 4b demonstrates the XRD spectra of the 100 nm layer thickness Cu/Ni samples at different annealing temperatures. Comparison of XRD patterns between the as-deposited and annealed states shows no obvious peak position change upon annealing, except a slight increase in peak height at higher annealing temperature, likely due to improved crystallinity. Although not included, the XRD spectra of the 200 nm and 25 nm layer thickness samples show similar behaviors—no clear temperature dependence.

Moving to Figure 5, the XRD spectra of the Cu/Al samples reveal distinct features. In the as-deposited Cu/Al multilayer samples (Figure 5a), a clear separation exists between the Cu (111) and Al (111) peaks. However, the co-sputtered Cu-Al sample forms intermetallic Al_2Cu_3 phases, altering the XRD spectrum. The peak near 44 degrees is likely a combination of Cu (111) and Al_2Cu_3 (102) peaks.

In Figure 5b,c, the XRD spectra of the 100 and 25 nm layer samples demonstrate that below 150 °C, there is no discernible difference between the as-deposited and the low-temperature-annealed states (100 °C and 125 °C), and the stability of the Cu (111) and Al (111) peaks is maintained. This stability explains the consistent hardness observed in Figure 3b. However, intermetallic Cu-Al phases begin to emerge at higher annealing temperatures. For the 100 nm layer thickness sample, two distinct intermetallic peaks are identified at 150 °C— CuAl_2 (110) and Cu_9Al_4 (330). The Cu_9Al_4 (330) peak becomes more pronounced at 175 °C, and dominates after 200 °C. At elevated annealing temperatures, the Cu (111) and CuAl_2 (110) peaks are no longer detectable.

The known greater diffusivity of Cu in Al compared to Al in Cu is likely responsible for the initial formation of the CuAl_2 phase when Cu saturates in Al [24,33]. At even higher temperatures (~175 °C), the $\text{Cu} + \text{CuAl}_2 \rightarrow \text{Cu}_9\text{Al}_4$ reaction occurs at the interfaces. A similar reaction happens in the Cu/Al 25 nm sample as well (Figure 5c). However, intermetallic formation occurs at a lower annealing temperature (100 °C) in the 25 nm samples than in the 100 nm samples, indicating faster diffusion of atoms in thinner layers even at a lower annealing temperature. In the co-sputtered Cu-Al thin film (Figure 5d), Cu_9Al_4 and $\epsilon\text{-Al}_2\text{Cu}_3$ phases are present in both the as-deposited and annealed states. The most significant disparity between the multilayer Cu/Al and co-sputtered Cu-Al samples is the abundant intermetallic phases observed in the as-deposited and thermally annealed co-sputtered sample.

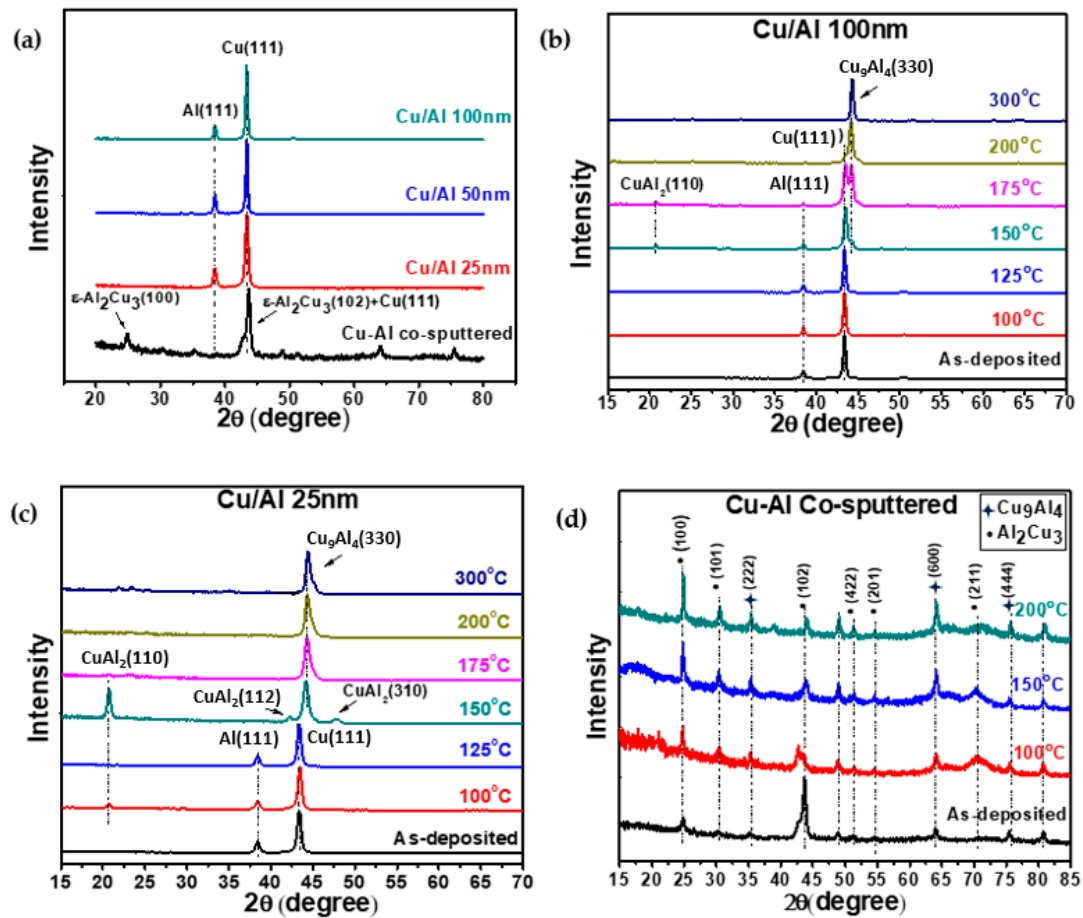


Figure 5. XRD spectra for Cu/Al thin films: as-deposited samples of different layer thickness (including the co-sputtered) (a); as-deposited and annealed samples: (b) individual layer thickness of 100 nm, (c) individual layer thickness of 25 nm, and (d) co-sputtered Cu-Al.

XRD analysis further supports the principle of post-deposition annealing strengthening, as evidenced by the presence of harder intermetallic phases (CuAl_2 and Cu_9Al_4) compared to pure Cu and Al. The reduced layer thicknesses of the 50 nm and 25 nm Cu/Al samples, when compared to the 100 nm Cu/Al sample, facilitates enhanced diffusion, leading to a more rapid and saturated increase in hardness. Notably, the co-sputtered Cu-Al samples exhibit a sufficient mixture of Cu and Al during the deposition process, resulting in the formation of intermetallic phases even at room temperature. Importantly, this intermetallic structure and the corresponding hardness are maintained after annealing, indicating a superior thermal stability of the co-sputtered system.

3.4. SEM Morphology of Annealed Samples

Annealed samples show distinct cross-sectional morphologies compared to their as-deposited counterparts. In Figure 6, cross-sectional SEM images of the 100 nm layer thickness Cu/Ni as-deposited sample and those annealed at 100 °C, 200 °C, and 300 °C reveal notable changes. The as-deposited sample displays a clear layer-by-layer structure. However, in samples annealed at higher temperatures, the Cu layer appears significantly thicker than in the as-deposited state. This effect is particularly pronounced in the 300 °C annealed sample, indicating increased diffusion between Cu and Ni layers with higher annealing temperatures.

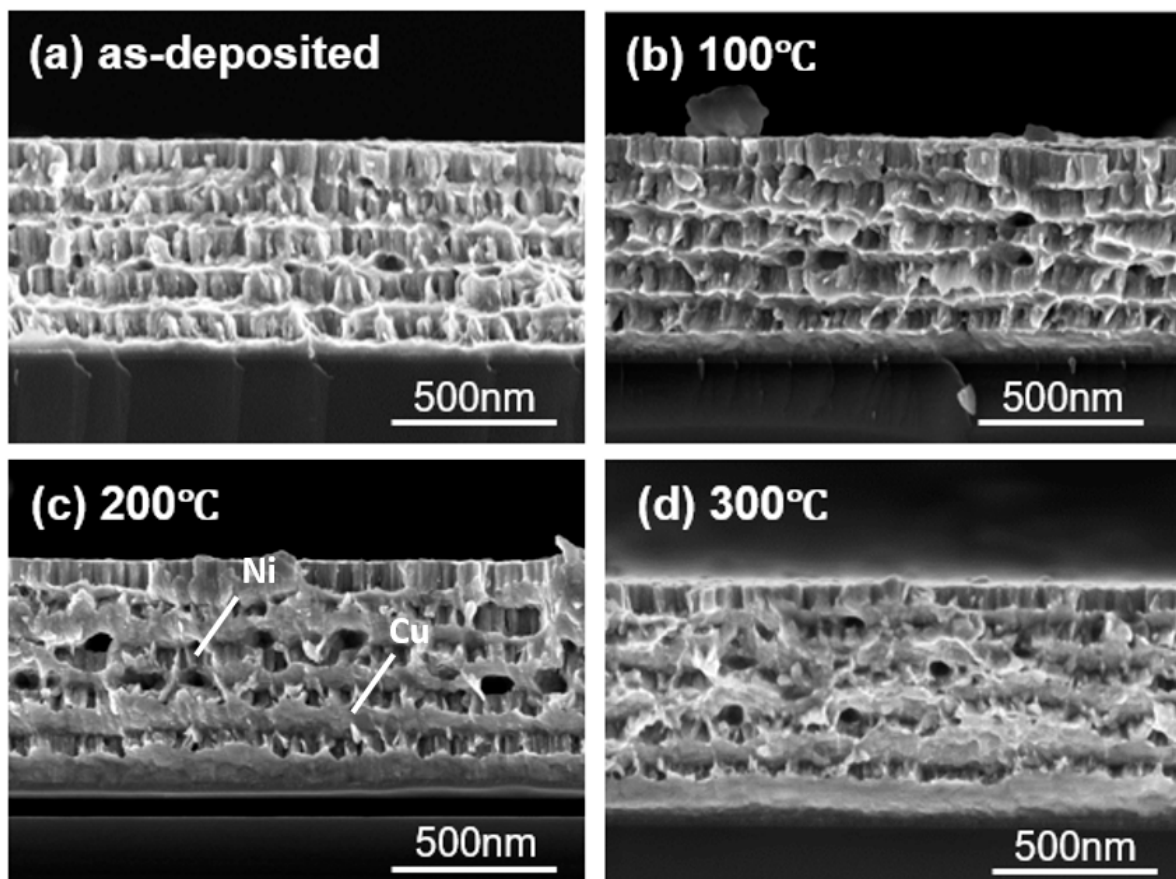


Figure 6. Cross-sectional SEM images of Cu/Ni 100 nm samples: (a) as-deposited, (b) 100 °C annealed, (c) 200 °C annealed, and (d) 300 °C annealed.

At low annealing temperatures (<100 °C), the cross-sectional SEM (Figure 6b) shows no obvious diffusion, suggesting that the enhanced mechanical properties may be attributed to grain boundary relaxation [8,34,35]. Annealing facilitates the transition of grain boundaries to a more ordered equilibrium state, hindering the movement of dislocations and enhancing hardness. However, at higher annealing temperatures (>100 °C), diffusion and solid solution formation induce deformation and the development of stress fields in the samples, potentially contributing to the hardness enhancement in the Cu/Ni multilayer thin film at elevated annealing temperatures.

Figure 7 presents cross-sectional images of the Cu/Al 100 nm sample with different annealing temperatures (125 °C to 300 °C). The first two images depict a clear layer-by-layer structure, aligning with the XRD-based conclusion that little diffusion occurs at annealing temperatures below 150 °C. The as-deposited and 125 °C annealed samples show undulating structures, likely due to the ductile deformation of Cu and Al during fracture. However, at annealing temperatures of 150 °C and 175 °C, the Cu layers become thinner due to diffusion. A further increase in annealing temperatures (200 °C and 300 °C) results in increasing intermixing of Cu and Al layers, explaining the different XRD peaks between the 300 °C annealed samples and the as-deposited ones. Additionally, the fractal cross-sections in Figure 7c–f become visibly smoother, providing additional evidence of the brittle intermetallic phase formation with increasing temperature.

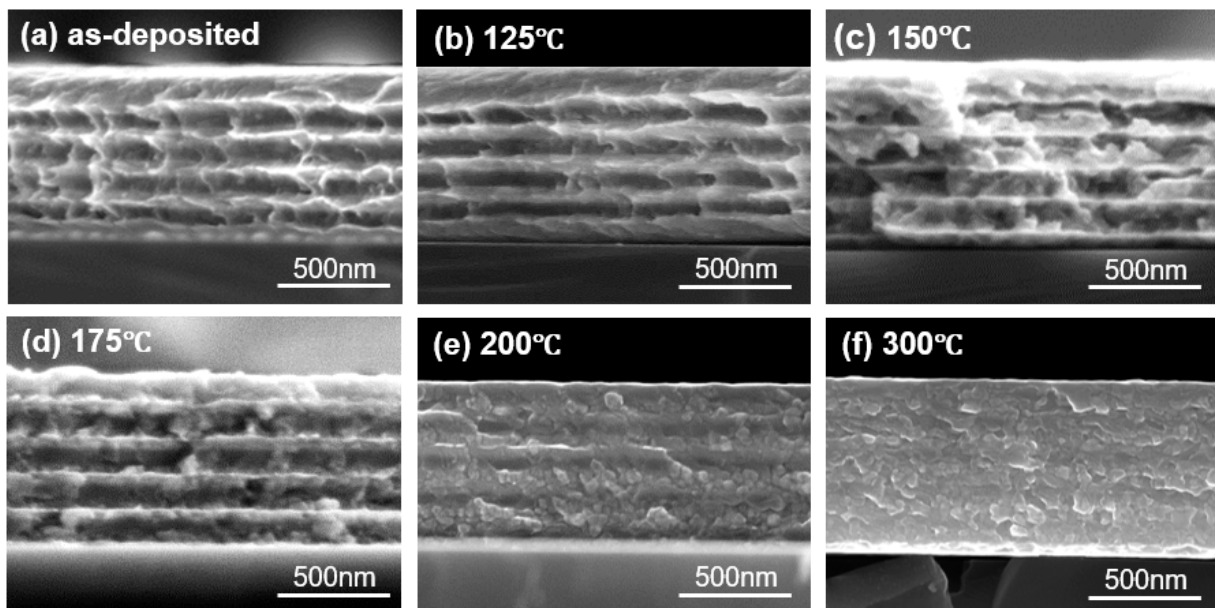


Figure 7. Cross-sectional SEM images of Cu/Al 100 nm samples: (a) as-deposited, and (b) 125 °C, (c) 150 °C, (d) 175 °C, (e) 200 °C, and (f) 300 °C annealed.

3.5. Discussion

This study delved into thermal-annealing-induced strengthening mechanisms within Cu/Ni and Cu/Al multilayer systems, encompassing individual layer thicknesses spanning 25 nm to 200 nm, and annealing temperatures from 100 °C to 300 °C. The correlation between increased hardness and decreasing layer thickness in the as-deposited samples affirmed the impact of layer thicknesses in metallic multilayers. With annealing, the Cu/Ni samples exhibited a gradual and modest increase in hardness, up to 30%, from room temperature to 300 °C, while the Cu/Al counterparts showcased a remarkable hardness surge of approximately 150%, within a specific temperature range between 125 °C and 200 °C. Interestingly, the Cu/Al samples displayed little temperature dependence below 125 °C or beyond 200 °C, maintaining consistent hardness. The co-sputtered Cu-Ni and Cu-Al samples consistently demonstrated higher hardness than their multilayered counterparts, albeit with distinctly different temperature dependence—the hardness of Cu-Ni increased with annealing temperature while Cu-Al maintained a constant high hardness throughout the entire temperature range.

While neither the XRD spectra nor the cross-sectional SEM revealed significant structural difference between the low-temperature-annealed and the as-deposited samples in Cu/Ni multilayers, observable diffusion became apparent at an annealing temperature of 200 °C. This diffusion of Cu and Ni layers at higher temperatures contributed to increased hardness through the formation of solid solutions, with the strengthening observed in low-temperature-annealed samples attributed to grain boundary relaxation.

Contrastingly, in Cu/Al multilayer samples, annealing induced a substantial hardness increase between 125 °C and 200 °C. XRD and cross-sectional SEM results indicated that annealing facilitated Cu diffusion into adjacent Al layers, forming various intermetallic phases (CuAl_2 and Cu_9Al_4) responsible for the significant increase in hardness. Notably, the as-deposited Cu-Al co-sputtered samples already exhibited rich intermetallic phases, reaching a hardness of ~11 GPa, which remained constant after annealing. As such, the hardness of the co-sputtered Cu-Al samples may be considered an asymptotic value for annealed Cu/Al multilayer systems.

Overall, the XRD spectra and SEM morphologies exhibit a strong correlation and play a crucial role in elucidating the observed change in hardness with varying annealing temperatures. The progressive rise in hardness within the Cu/Ni system can be attributed

to a combination of grain boundary relaxation and thermal diffusion between the Cu and Ni elements, facilitating the formation of a solid solution. On the other hand, the abrupt increase in hardness observed in the Cu/Al system is associated with the formation of district Cu-Al intermetallic phases.

4. Conclusions

This study illustrates distinct thermal strengthening mechanisms between the two metallic multilayer systems as well as their corresponding co-sputtered counterparts: solid solution strengthening in Cu/Ni and intermetallic strengthening in Cu/Al. The results underscore the pivotal roles played by layer thickness and annealing conditions in influencing the diffusion kinetics and subsequent formation of solid solution and intermetallic phases, ultimately shaping the mechanical properties of the materials. Additionally, the ability of co-sputtering Cu-Al samples to form and retain intermetallic phases even at low temperatures suggests a unique advantage in achieving desired material characteristics, contributing to the overall understanding of the relationship between microstructure, phase evolution, and mechanical behavior in multilayered and co-sputtered systems. The insights gained from this work will serve as valuable guidance for the future design and application of engineered multilayer materials, underscoring their potential in tailoring specific material properties for various applications.

Author Contributions: Conceptualization, J.W.; Methodology, Y.Z. and J.W.; Formal Analysis, Y.Z.; Investigation, Y.Z.; Resources, J.W.; Data Curation, Y.Z.; Writing—Original Draft, Y.Z.; Writing—Review and Editing, J.W.; Supervision, J.W. All authors have read and agreed to the published version of the manuscript.

Funding: The authors acknowledge the financial support by the University of Washington Royal Research Fund (grant no. 68-2003). Part of this work was conducted at the University of Washington Molecular Analysis Facility, which is supported in part by funds from the Molecular Engineering & Sciences Institute, the Clean Energy Institute, and the National Science Foundation (NNCI-2025489 and NNCI-1542101).

Data Availability Statement: The original contributions presented in the study are included in the article, further inquiries can be directed to the corresponding author.

Conflicts of Interest: The authors declare no conflict of interest.

References

1. Moleinia, Z.; Bahr, D.F. Multi-Scale Analyses and Modeling of Metallic Nano-Layers. *Materials* **2021**, *14*, 450. [[CrossRef](#)]
2. Wang, K.; Cai, W. Modeling the effects of individual layer thickness and orientation on the tribocorrosion behavior of Al/Cu nanostructured metallic multilayers. *Wear* **2021**, *477*, 203849. [[CrossRef](#)]
3. Daghbouj, N.; Sen, H.; Čížek, J.; Lorinčík, J.; Karlík, M.; Callisti, M.; Čech, J.; Havránek, V.; Li, B.; Krsjak, V.; et al. Characterizing heavy ions-irradiated Zr/Nb: Structure and mechanical properties. *Mater. Des.* **2022**, *219*, 110732. [[CrossRef](#)]
4. Niu, T.; Zhang, Y.; He, Z.; Sun, T.; Richter, N.A.; Wang, H.; Zhang, X. Texture development in Cu-Ag-Fe triphase immiscible nanocomposites with superior thermal stability. *Acta Mater.* **2023**, *244*, 118545. [[CrossRef](#)]
5. Nasim, M.; Li, Y.; Wen, C. Individual layer thickness-dependent nanoindentation and nanotribological behaviors of Ta/Co nanolaminates. *Tribol. Int.* **2020**, *156*, 106845. [[CrossRef](#)]
6. Liang, Y.; Luo, A.; Yang, L.; Zhao, J.; Wang, L.; Wan, Q. Effect of interface structure and layer thickness on the mechanical properties and deformation behavior of Cu/Ag nanolaminates. *Phys. B Condens. Matter* **2023**, *661*, 414933. [[CrossRef](#)]
7. Yang, Z.; Wang, J. Deposition Temperature Induced Texture and Strengthening of Ti/Ni Multilayer Thin Films. *J. Appl. Mech.* **2023**, *90*, 121005. [[CrossRef](#)]
8. Yang, Z.; Wang, J. Orientation-Dependent Hardness in As-Deposited and Low-Temperature Annealed Ti/Ni Multilayer Thin Films. *J. Appl. Mech.* **2015**, *82*, 011008. [[CrossRef](#)]
9. Yang, Z.; Wang, J. Coupled annealing temperature and layer thickness effect on strengthening mechanisms of Ti/Ni multilayer thin films. *J. Mech. Phys. Solids* **2016**, *88*, 72–82. [[CrossRef](#)]
10. Misra, A.; Göken, M.; Mara, N.A.; Beyerlein, I.J. Hierarchical and heterogeneous multiphase metallic nanomaterials and laminates. *MRS Bull.* **2021**, *46*, 236–243. [[CrossRef](#)]
11. Friedman, L.H. Exponent for Hal—Petch behaviour of ultra-hard multilayers. *Philos. Mag.* **2006**, *86*, 1443–1481. [[CrossRef](#)]
12. Kaneko, Y.; Mizuta, Y.; Nishijima, Y.; Hashimoto, S. Vickers hardness and deformation of Ni/Cu nano-multilayers electrodeposited on copper substrates. *J. Mater. Sci.* **2005**, *40*, 3231–3236. [[CrossRef](#)]

13. Misra, A.; Hirth, J.P.; Kung, H. Single-dislocation-based strengthening mechanisms in nanoscale metallic multilayers. *Philos. Mag. A-Phys. Condens. Matter Struct. Defects Mech. Prop.* **2002**, *82*, 2935–2951. [[CrossRef](#)]
14. Li, Q.; Anderson, P.M. Dislocation-based modeling of the mechanical behavior of epitaxial metallic multilayer thin films. *Acta Mater.* **2005**, *53*, 1121–1134. [[CrossRef](#)]
15. Jian, W.-R.; Xu, S.; Su, Y.; Beyerlein, I.J. Role of layer thickness and dislocation distribution in confined layer slip in nanolaminated Nb. *Int. J. Plast.* **2022**, *152*, 103239. [[CrossRef](#)]
16. Ji, W.; Jian, W.-R.; Su, Y.; Xu, S.; Beyerlein, I.J. Role of stacking fault energy in confined layer slip in nanolaminated Cu. *J. Mater. Sci.* **2023**. [[CrossRef](#)]
17. Fani, M.; Jian, W.-R.; Su, Y.; Xu, S. Confined Layer Slip Process in Nanolaminated Ag and Two Ag/Cu Nanolaminates. *Materials* **2024**, *17*, 501. [[CrossRef](#)] [[PubMed](#)]
18. Hoagland, R.G.; Mitchell, T.E.; Hirth, J.P.; Kung, H. On the strengthening effects of interfaces in multilayer fcc metallic composites. *Philos. Mag. A-Phys. Condens. Matter Struct. Defects Mech. Prop.* **2002**, *82*, 643–664. [[CrossRef](#)]
19. Hoagland, R.; Kurtz, R.; Henager, C. Slip resistance of interfaces and the strength of metallic multilayer composites. *Scr. Mater.* **2004**, *50*, 775–779. [[CrossRef](#)]
20. Beyerlein, I.J.; Li, Z.; Mara, N.A. Mechanical properties of metal nanolaminates. *Annu. Rev. Mater. Res.* **2022**, *52*, 281–304. [[CrossRef](#)]
21. Wang, J.; Hoagland, R.; Hirth, J.; Misra, A. Atomistic modeling of the interaction of glide dislocations with “weak” interfaces. *Acta Mater.* **2008**, *56*, 5685–5693. [[CrossRef](#)]
22. Li, J.; Chen, Y.; Xue, S.; Wang, H.; Zhang, X. Comparison of size dependent strengthening mechanisms in Ag/Fe and Ag/Ni multilayers. *Acta Mater.* **2016**, *114*, 154–163. [[CrossRef](#)]
23. Liu, Y.; Bufford, D.; Wang, H.; Sun, C.; Zhang, X. Mechanical properties of highly textured Cu/Ni multilayers. *Acta Mater.* **2011**, *59*, 1924–1933. [[CrossRef](#)]
24. Zhou, Q.; Li, S.; Huang, P.; Xu, K.W.; Wang, F.; Lu, T.J. Strengthening mechanism of super-hard nanoscale Cu/Al multilayers with negative enthalpy of mixing. *APL Mater.* **2016**, *4*, 096102. [[CrossRef](#)]
25. Wei, X.; Zhou, Q.; Xu, K.; Huang, P.; Wang, F.; Lu, T. Enhanced hardness via interface alloying in nanoscale Cu/Al multilayers. *Mater. Sci. Eng. A* **2018**, *726*, 274–281. [[CrossRef](#)]
26. Gupta, K.P. The Cu-Ni-Ti (Copper-Nickel-Titanium) system. *J. Phase Equilibria Diffus.* **2002**, *23*, 541–547. [[CrossRef](#)]
27. Massalski, T.B.; Okamoto, H. *Binary Alloy Phase Diagrams*; ASM International: Materials Park, OH, USA, 1990.
28. Barshilia, H.C.; Rajam, K. Characterization of Cu/Ni multilayer coatings by nanoindentation and atomic force microscopy. *Surf. Coatings Technol.* **2002**, *155*, 195–202. [[CrossRef](#)]
29. Sun, Y.; Chen, Y.; Tsuji, N.; Guan, S. Microstructural evolution and mechanical properties of nanostructured Cu/Ni multilayer fabricated by accumulative roll bonding. *J. Alloys Compd.* **2020**, *819*, 152956. [[CrossRef](#)]
30. Ito, T.; Yamamoto, R.; Yoshihara, A. Mechanical-Properties of Cu/Al Multilayered Thin-Films. *Surf. Coatings Technol.* **1991**, *45*, 215–220. [[CrossRef](#)]
31. McDonald, I.G.; Moehlenkamp, W.M.; Arola, D.; Wang, J. Residual stresses in Cu/Ni Multilayer thin films measured using the $\sin^2\psi$ method. *Exp. Mech.* **2019**, *59*, 111–120. [[CrossRef](#)]
32. Oliver, W.C.; Pharr, G.M. An improved technique for determining hardness and elastic-Modulus using load and displacement sensing indentation experiments. *J. Mater. Res.* **1992**, *7*, 1564–1583. [[CrossRef](#)]
33. Honarpisheh, M.; Asemabadi, M.; Sedighi, M. Investigation of annealing treatment on the interfacial properties of explosive-welded Al/Cu/Al multilayer. *Mater. Des.* **2012**, *37*, 122–127. [[CrossRef](#)]
34. Zeng, D.; Li, J.; Shi, Y.; Li, X.; Lu, K. Thermally-triggered grain boundary relaxation in a nanograined Ni-Mo-W alloy. *Nano Res.* **2023**, *16*, 12800–12808. [[CrossRef](#)]
35. Rodríguez, A.M.; Bozzolo, G.; Ferrante, J. Multilayer relaxation and surface energies of Fcc and Bcc metals using equivalent crystal theory. *Surf. Sci.* **1993**, *289*, 100–126. [[CrossRef](#)]

Disclaimer/Publisher’s Note: The statements, opinions and data contained in all publications are solely those of the individual author(s) and contributor(s) and not of MDPI and/or the editor(s). MDPI and/or the editor(s) disclaim responsibility for any injury to people or property resulting from any ideas, methods, instructions or products referred to in the content.